OBSERVATIONAL EVIDENCE FOR POLAR SPOTS

KLAUS G. STRASSMEIER
Institut für Astronomie
Universität Wien
Türkenschanzstraße 17
A-1180 Wien, Austria

Abstract. "Are results from ill-posed problems, like Doppler-imaging, conclusive at all?" and "Could polar spots be simple image-reconstruction artifacts?" are often asked questions. Although I can not definitively answer them, I will present observational evidence for the existence of cool starspots at or very near a stellar rotation pole.

1. Introduction

The notion of polar spots stems from the first Doppler image of HR 1099 by Vogt & Penrod (1983) and has been confirmed now for 18 out of 27 late-type stars with Doppler maps (see Appendix Table 1). Despite that these maps were generated by seven different groups of investigators two major points of criticism remain:

- All information on polar spots comes from Doppler imaging which itself is based on the periodic variations in spectral line profiles. The inversion of these line profiles to a two-dimensional temperature image needs information on the "undisturbed" shape and strength of the local line profile: *what if the adopted local line profile is incorrect?*
- *"Why doesn't the Sun show polar spots?"* is the obvious second point of criticism — although more a phenomenological one than one against polar starspots, but nevertheless a "nasty" question!

We are just at the beginning of our understanding of the formation of polar spots on rapidly-rotating stars (see Schüssler, this proceedings). We simply do not know enough yet to actually make *observable predictions*, and I feel

K. G. Strassmeier and J. L. Linsky (eds.), Stellar Surface Structure, 289–298.

we should first summarize current observational results before attempting answering the above questions.

2. A brief survey of Doppler images

Table 1 lists all published (photospheric) Doppler images of late-type stars (several more are currently in work), their time of observation, the variable type and M-K classification, rotation parameters, the amplitude of the lightcurve in case this information is used for the Doppler map, the inclination i of the stellar rotation axis and whether a polar spot (P), or high-latitude (H) or low-latitude (L) spots were seen. The 27 stars in Table 1 consist of 12 RS CVn binaries, 4 T Tauri objects, 3 FK Comae stars, 2 W UMa contact systems, 4 young single dwarf stars, and 2 BY Draconis binary. Their rotation periods range between 19.4 days for the K1 giant σ Gem to the 0.31 days of the G2V W-UMa system YY Eri. Respectively, the unprojected equatorial rotational velocities range from 165 $\mathrm{km\,s^{-1}}$ for FK Comae to 26 $\mathrm{km\,s^{-1}}$ for II Peg. Furthermore, almost all evolutionary stages are present: from classical and weak-lined T Tauri stars to evolved MK-class III giants, singles and binaries, the latter with and without mass transfer. Consequently, a wide range of stellar radii has been observed: between the 0.77 $\mathrm{R_\odot}$ for the dM1e stars in YY Gem to the 16 $\mathrm{R_\odot}$ of YY Men. Finally, the effective surface temperatures of the stars in Table 1 span from an estimated cool 4000 K for DF Tau and YY Gem to a warm 6000 K for the W-UMa system AE Phe.

3. Evidence from line-profile modeling

3.1. THE QUEST FOR CORRECT TRANSITION PROBABILITIES

Figure 1 presents several line-profile fits to the observed solar Ca I 6439.075-Å line taken from Kurucz's et al. (1984) solar atlas. The theoretical profiles were computed with the solar model of Kurucz (1991) (5770 K, $\log g = 4.55$, $\mathrm{He/H} = 0.1$, $\xi = 1.0\ \mathrm{km\,s^{-1}}$), and his most recent line list, incorporating altogether 40 million lines. The line-synthesis program of Stift (1995) is being used to compute chunks of spectra from a solution of the equation of transfer from a grid of 72 depth points including micro- and macroturbulence as well as rotation.

The only parameters left for fitting the solar profiles were the transition probabilities ($\log gf$) of the mapping lines and their blends. Our best estimates are (in parenthesis: our $\log gf$ value | Kurucz-CD value): Ca I 6439.075 (+0.47|+0.47), Fe I 6430.852 (-1.85|-1.85), Fe I 6411.647 (-0.32|-0.82), Fe I 6393.602 (-1.50|-1.62), Li I 6707.850 (+0.18|+0.18). Obviously, the $\log gf$'s used for imaging are not so unrealistic as sometimes said – and

https://doi.org/10.1017/S0074180900083303 Published online by Cambridge University Press

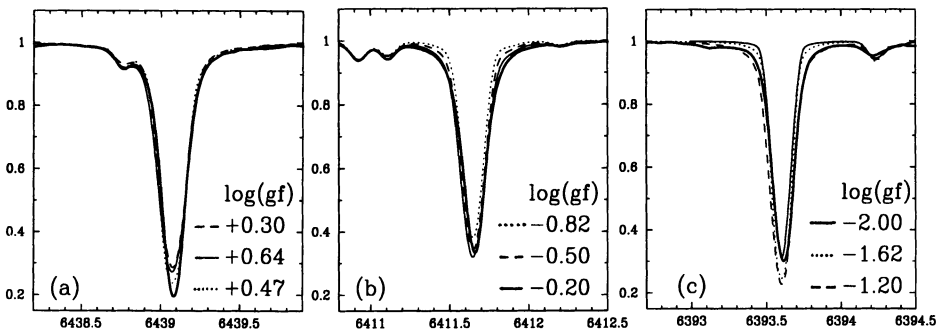

Figure 1. Examples of our comparison of theoretical line profiles with the observed solar spectrum. Left: Ca I 6439.075. Middle: Fe I 6411.647. Right: Fe I 6393.602.

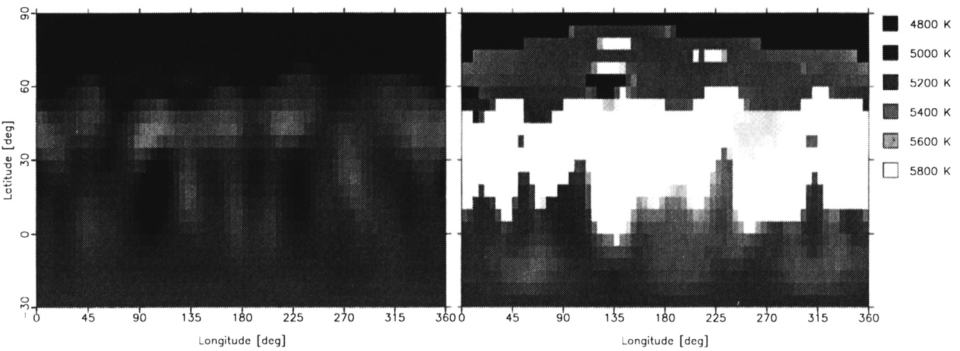

Figure 2. Two Ca I Doppler maps of HD 199178 reconstructed with incorrect transition probabilities: $\log gf = +0.30$ (left) and $+0.64$ (right) instead of $+0.47$.

this fact strengthens the reliability of Doppler maps and consequently the existence of polar spots.

No depth dependence of microturbulence could be taken into account in our computations, which might explain part of the misfit of the core of the strong Ca I line and of the wings in the weaker lines. The C-type asymmetry of both solar lines in Fig. 1 (thick line) is the typical result of surface convection in granular cells. Note that the theoretical Ca lines are too *shallow* for the observed solar line depth and would – if severely enhanced in active stars – produce the *opposite* effect than a polar spot!

Figure 2 presents two Doppler maps of HD 199178 reconstructed from "real" data with all their intrinsic faults, like incomplete phase coverage or possible errors in the continuum setting, but computed with wrong transition probabilities ($\log gf = +0.64$ and $+0.30$ instead of $+0.47$). A weaker $\log gf$ has – at least in the case of Ca I 6439 – only little influence on the

https://doi.org/10.1017/S0074180900083303 Published online by Cambridge University Press

generated map (the χ^2 of the line-profile fit is 0.039, almost identical to the fit with +0.47) corresponding to the map in Fig. 2 (left), while a stronger $\log gf$ has a disastrous effect on the reconstructed map (the χ^2 of the fit is 0.109) because the local profiles become too broad and the code is forced to put a hot band around the star (Fig. 2 right). Amazingly though, and this is the point of the whole exercise, a polar spot is still recovered!

3.2. UNKNOWN ELEMENTAL ABUNDANCES

Could an incorrectly adopted abundance result in a spurious polar spot? And how different could the abundance be to be neglected in the line-profile inversion? Figure 3 compares two Doppler maps for HD 199178 from Ca I 6439, one with "correct" abundance (−5.15) and one with an artificial overabundance of 0.2 dex. Both maps were computed from altogether eight blends with equivalent widths between 3 and 15 mÅ. Once again, the polar spot is clearly recovered and needed by the data. Note that an artificial underabundance would actually strengthen a polar cap-like feature.

3.3. BLENDED LINE PROFILES

Unruh & Cameron (1995) already showed that the neglect of blends in the wings of the mapping line could lead to spurious banding at high latitudes, and eventually to a polar-spot look-alike if the equivalent width of the blend is large enough. However, these were model calculations. What about real observations? Figure 4 shows two Ca I-6439 maps of HD 199178. Both were reconstructed without blends. One with "correct" abundance and the other with an overabundance of again 0.2 dex. The missing equivalent width due to the blends is thereby compensated for with the artificial overabundance. A polar spot is the result in any case.

3.4. DEPENDENCE OF LINE STRENGTH ON TEMPERATURE

The most recent images listed in Table 1 were already generated by taking into account that the local line profile from a spot is different than from the surrounding warmer photosphere. Again, polar spots were reconstructed e.g. for HR 1099! For further details on the temperature dependence of spectral lines see the articles of Gray (this proceedings) and Stift & Strassmeier (1995).

3.5. DO WE USE THE CORRECT MICROTURBULENCE?

Figure 5 compares three synthetic Ca I 6439 line profiles from a $T_{\rm eff} = 5500$ and $\log g = 2.5$ model atmosphere and microturbulences of ξ =0, 1, and 2

https://doi.org/10.1017/S0074180900083303 Published online by Cambridge University Press

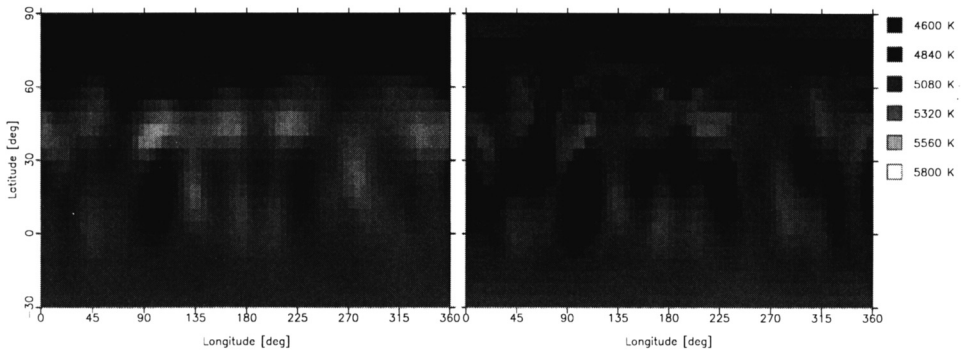

Figure 3. Doppler images of HD 199178 with "correct" input abundance (left image) and an artificial overabundance of 0.2 dex (right image). Both images were computed from Ca I 6439-Å including eight blends.

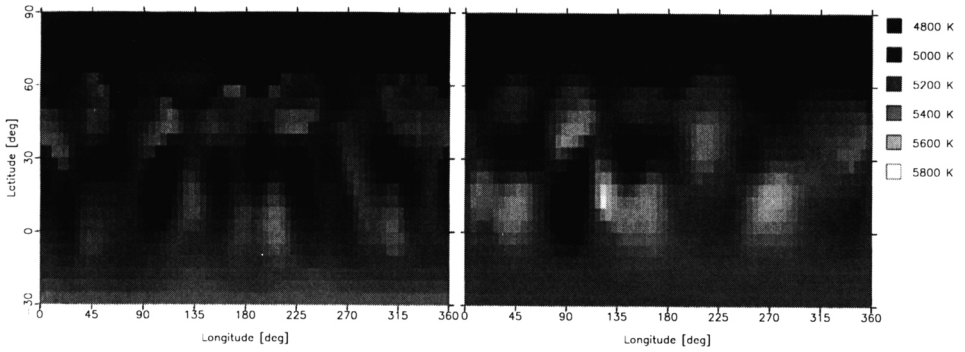

Figure 4. Doppler images of HD 199178 reconstruced from the same data set as in Fig. 2 but without blends. *Left:* with correct abundances. *Right:* with an artificial overabundance of 0.2 dex.

$\mathrm{km\,s^{-1}}$. In Fig. 5 notice the different profile shape for the very weak line, an Fe I line to the blue of the Ca I line, and the strong Ca I 6439 line! So we may suspect that a wrongly adopted microturbulence has a profound effect on our reconstructed Doppler image. But does it especially affect the stellar polar regions? Figure 6 is a reconstruction of the same set of observations of HD 199178 as in Figs. 2, 3 and 4 but without microturbulence at all. One map is with correct $\log gf$ (+0.47) and the other with an abnormally large $\log gf$ (+0.64). The latter was obtained by optimizing the quality of the profile fit but in no case, however, got the χ^2 closer to the "correct" line-profile fit (with ξ=2 $\mathrm{km\,s^{-1}}$) than roughly a factor two. Due to the smaller equivalent width of the local line profile the inversion code comes up with a generally cooler surface to compensate for the missing equivalent

https://doi.org/10.1017/S0074180900083303 Published online by Cambridge University Press

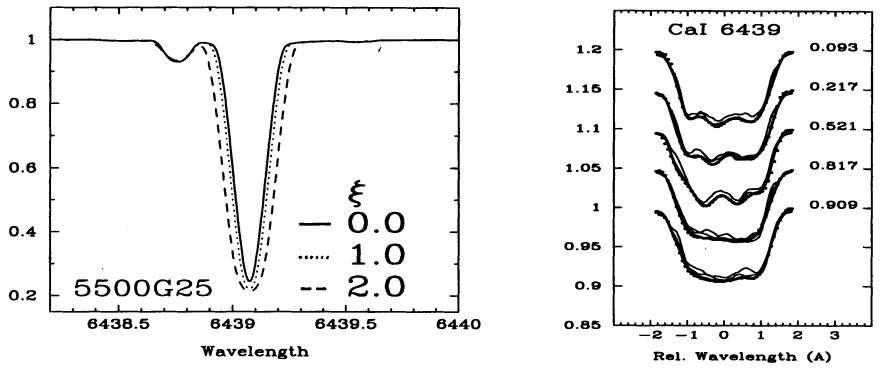

Figure 5. *Left:* The effect of microturbulence ξ on the Ca I 6439 line. *Right:* HD 199178 fits with zero microturbulence and correct $\log gf$ (thin line: worst fit), a too large a $\log gf$ of +0.64 (thin line: slightly better fit) and the best fit with ξ=2 km s^{-1} and $\log gf$=+0.47 (thick line). The dots are the observations.

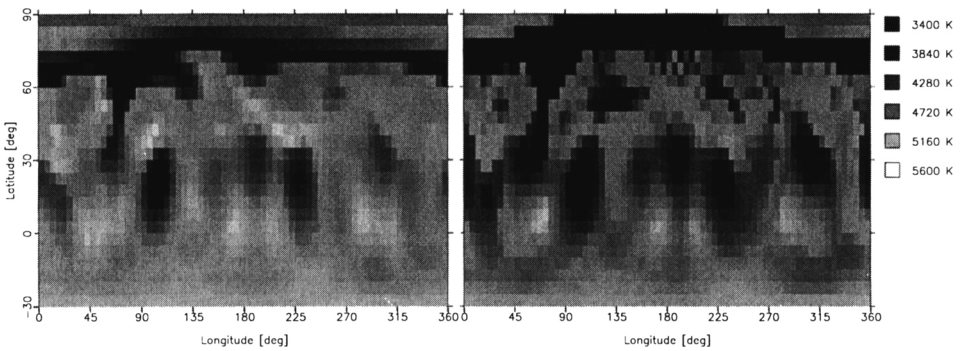

Figure 6. Doppler images of HD 199178 reconstructed with zero microturbulence and correct $\log gf$ (left) and too strong a $\log gf$ (right), respectively.

width (note the different temperature scales in Fig. 6).

Actually, a cool polar feature is reconstructed for HD 199178 fairly independent of the adopted microturbulence. The cap-like structure, however, changes to something like a circumpolar ring when a grossly incorrect $\log gf$ *and* ξ are used.

3.6. INTRINSIC SPOT VARIABILITY

All previously discussed line-profile complications could only show up as a *symmetric* effect in a Doppler image – for example a circular polar cap or an equatorial ring. Wouldn't it be nice evidence for the reality of polar spots if we had mapped a star at different times with the same mapping code and

https://doi.org/10.1017/S0074180900083303 Published online by Cambridge University Press

found a polar spot at a particular time and none at some other time? Well, this is exactly the case for the K2 dwarf star LQ Hya (see Table 1) where Saar et al. (1994) reconstructed an asymmetric polar spot in March 1993 but not in May and February 1991 (neither did our own map from February 1991). Obviously, the line profile models couldn't be the cause of the polar feature in 1993. Furthermore, long term variations in the asymmetry of the persistent polar spot of HR 1099 (see Vogt & Hatzes, this proceedings) are additional evidence of its reality. How could a time-independent symmetric fault produce a time-dependent asymmetric artifact?

3.7. DEPENDENCE OF THE PROFILE SHAPE ON INCLINATION

Hatzes et al. (1995) presented a poster at this meeting that dealt with a possible dependence of the shape of observed average line profiles with the inclination of the stellar rotation axis: the more inclined, the flatter the observed line profile. If proven correct, it is further evidence for the existence of polar spots. Our Table 1 tells us that all stars with $i \leq 45°$ were reconstructed with a polar spot (except the single attempt by Gondoin (1986) for HR 1099) and thus strengthens Hatzes's conjecture.

Other (secondary) evidence has been presented – mainly from long-term photometry – by, e.g., Oláh et al. (1992)(1991) for HK Lac and V833 Tau, by Pettersen et al. (1992) for BY Dra and EV Lac, by Dempsey et al. (1992) for HD 199178 and HR 1099, by Strassmeier (1990) for EI Eri.

Acknowledgements: It's a pleasure to thank John Rice for numerous discussions on the mapping topic, especially during our long Hawaiian nights, Kolya Piskunov for providing the numerical data of Kurucz's NSO solar atlas, and Steve Vogt for refereeing this paper.

References

Collier Cameron A., 1995, MNRAS 275, 534
Collier Cameron A., Unruh Y. C., 1994, MNRAS 269, 814
Dempsey R. C., Bopp B. W., Strassmeier K. G., Granados A. F., Henry G. W., Hall D. S., 1992, ApJ 392, 187
Donati J. F., Brown S. F., Semel M. et al., 1992, A&A 265, 682
Gondoin P., 1986, A&A 160, 73
Hatzes A. P., 1993, ApJ 410, 777
Hatzes A. P., 1995a, AJ 109, 350
Hatzes A. P., 1995b, in Strassmeier K. G. (ed), *Poster Proceedings: Stellar Surface Structure*, IAU Symp. 176, Univ. Vienna, p. 87
Hatzes A. P., 1995c, in Strassmeier K. G. (ed), *Poster Proceedings: Stellar Surface Structure*, IAU Symp. 176, Univ. Vienna, p. 90
Hatzes A. P., 1995d, ApJ 451, 784
Hatzes A. P., Vogt S. S., Ramseyer T. F., Misch A., 1995, in Strassmeier K. G. (ed), *Poster Proceedings: Stellar Surface Structure*, IAU Symp. 176, Univ. Vienna, p. 9
Hatzes A. P., Vogt S. S., 1992, MNRAS 258, 387

Hempelmann A., Hatzes A. P., Kürster M., Patkós L., 1995, in Strassmeier K. G. (ed), *Poster Proceedings: Stellar Surface Structure*, IAU Symp. 176, Univ. Vienna, p. 194
Hubl B., Strassmeier K. G., 1995, in Strassmeier K. G. (ed), *Poster Proceedings: Stellar Surface Structure*, IAU Symp. 176, Univ. Vienna, p. 96
Jankov S., Donati J.-F., 1995, in Huang L. et al. (eds), Proc. of the 4th Workshop on MUSICOS, ESA-ESTEC, p. 143
Joncour I., Bertout C., Bouvier J., 1994a, A&A 291, L19
Joncour I., Bertout C., Menard F., 1994b, A&A 285, L25
Kurucz R. L., 1991, in Davis Philip A. G., et al. (eds), *Precision Photometry: Astrophysics of the Galaxy*, Schenectady, Davis, p. 27
Kurucz R. L., Furenlid I., Brault J., Testerman L., 1984, *Solar Flux Atlas from 296 to 1300 nm*, NSO Atlas No. 1
Kürster M., Dennerl K., 1993, in Linsky J. F. & Serio S. (eds), *Physics of Solar and Stellar Coronae*, Kluwer Academic Publishers, Netherlands, p. 443
Kürster M., Hatzes A. P., Pallavicini R., Randich S., 1992, in Giampapa M. S. & Bookbinder J. A. (eds.), Seventh Cambridge Workshop, *Cool Stars, Stellar Systems, and the Sun*, PASPC 26, p. 249
Kürster M., Schmitt J. H. M. M., Cutispoto G., 1994, A&A 289, 899
Maceroni C., Vilhu O., van't Veer, F., Van Hamme W., 1994, A&A 288, 529
Noah P. V., Bopp B. W., Fekel F., 1987, in Linsky J. L. & Stencel R. E. (eds), Fifth Cambridge Workshop, *Cool Stars, Stellar Systems, and the Sun*, Springer, p.506
Oláh K., Budding E., Butler C. J., Houdebine E. R. et al., 1992, MNRAS 259, 302
Oláh K., Pettersen B. R., 1991, A&A 242, 443
Petrov P. P., Gullbring E., Gahm G., et al., 1995, in Strassmeier K. G. (ed), *Poster Proceedings: Stellar Surface Structure*, IAU Symp. 176, Univ. Vienna, p. 217
Pettersen B. R., Olah K., Sandmann W. H., 1992, A&AS 96, 497
Piskunov N. E., Huenemoerder D. P., Saar S. H., 1994, in Caillault J. P. (ed), Eight Cambridge Workshop, *Cool Stars, Stellar Sytems, and the Sun*, PASPC 64, p. 658
Piskunov N. E., Tuominen I., Vilhu O., 1990, A&A 230, 363
Ramseyer T. F., Hatzes A. P., Jablonski F., 1995, AJ 110, 1364
Rice J. B., Strassmeier K.G., 1996, A&A, (in press)
Saar S. H., Piskunov N. E., Tuominen I., 1994, in Caillault J. P. (ed), Eight Cambridge Workshop, *Cool Stars, Stellar Systems, and the Sun*, PASPC 64, p. 661
Stift M. J., 1995, private comm.
Stift M. J., Strassmeier K. G., 1995, in Strassmeier K. G. (ed), *Poster Proceedings: Stellar Surface Structure*, IAU Symp. 176, Univ. Vienna, p. 29
Stout N., Vogt S. S., 1996, this proceedings
Strassmeier K. G., 1990, ApJ 348, 682
Strassmeier K. G., 1994, A&A 281, 395
Strassmeier K. G., 1996, A&A, (in press)
Strassmeier K. G., Rice J. B., Wehlau W. H. et al., 1991, A&A 247, 130
Strassmeier K. G., Rice J. B., Wehlau W. H. et al., 1993, A&A 268, 671
Strassmeier K. G., Welty A. D., Rice J. B., 1994, A&A 285, L17
Strassmeier K. G., Dempsey R. C., Rice J. B., 1996, A&A (submitted)
Unruh Y. C., Collier-Cameron A., Guenther E., 1995, in Strassmeier K. G. (ed), *Poster Proceedings: Stellar Surface Structure*, IAU Symp. 176, Univ. Vienna, p. 93
Unruh Y. C., Collier Cameron A., 1995, MNRAS 273, 116
Vogt S. S., 1988, in Carel de Strobel G. & Spite M. (eds.), IAU Symp. 132, *The Impact of Very High S/N Spectroscopy on Stellar Physics*, Kluwer Academic Publishers, p.253
Vogt S. S., Hatzes A. P., 1990, in Tuominen I., Moss D., Rüdiger G. (eds), IAU Coll. 130, *The Sun and Cool Stars: Activity, Magnetism, Dynamos*, Springer Verlag, p. 297
Vogt S. S., Hatzes A. P., 1996, this proceedings
Vogt S. S., Penrod G. D., 1983, PASP 95, 565

TABLE 1. A list of Doppler images of late-type stars

Star Year(s) of obs.	Type ΔV	M-K class i	$v \sin i$ Spots[1]	$P_{\rm rot}$ Reference
σ Gem	RS CVn	K1 III	27 km s^{-1}	19.4 d
1991-92	0.17 mag	60°	H, L	Hatzes (1993)
HU Vir	RS CVn	K0 III-IV	25 km s^{-1}	10.4 d
1991-92	0.25 mag	65°	P, H	Strassmeier (1994)
YY Men	FK Com	K2 III	50 km s^{-1}	9.55 d
Jan 1987	0.3 mag	65°	H, L	Piskunov et al. (1990)
Sep 1990	...	35°	P, L	Kürster & Dennerl (1993)
DF Tau	cTTS	M0	25 km s^{-1}	8.5 d
Nov 1994	...	60°	L	Unruh et al. (1995)
DM UMa	RS CVn	K0-1 IV-III	26 km s^{-1}	7.50 d
Jan 1993	0.2 mag	40°	P, L	Hatzes (1995a)
II Peg	RS CVn	K2 IV-V	24 km s^{-1}	6.72422 d
1992-94	0.25 mag	65°	P, H, L	Hatzes (1995b)
UX Ari	RS CVn	K0 IV	39 km s^{-1}	6.44 d
1983-84	0.3 mag	60°	H, L	Noah et al. (1987)
1986	...	60°	P, L	Vogt & Hatzes (1990)
IN Com	RS CVn	G5 III-IV	67 km s^{-1}	5.92 d
Mar 1994	0.02 mag	45°	P, L	Hubl & Strassm. (1995)
UZ Lib	RS CVn	K0 III	69 km s^{-1}	4.74 d
Mar 1994	0.35 mag	30°	P, L	Strassmeier (1996)
HD 199178	FK Com	G5 III-IV	71.5 km s^{-1}	3.3129 d
1985	...	80°	P, L	Vogt (1988)
1988-90	0.07 mag	30°	P, H, L	Strassmeier et al. (1996)
SU Aur	TTS	G2(III)	64 km s^{-1}	3.094 d
Nov 1994	...	80°	L	Petrov et al. (1995)
V711 Tau	RS CVn	K1 IV	41 km s^{-1}	2.84 d
Oct 1981	0.2 mag	33°	P, L	Vogt & Penrod (1983)
Sep 1983	...	33°	H	Gondoin (1986)
1984-85	...	33°	P, L	Vogt (1988)
1988-91	0.1 mag	33°	P, L	Donati et al. (1992)
Dec 1989	0.1 mag	33°	P, L	Jankov & Donati (1995)
Dec 1992	0.06 mag	33°	P, L	Jankov & Donati (1995)
1984-95	...	33°	P, L	Vogt & Hatzes (1996)
CF Tuc	RS CVn	K4 IV	35 km s^{-1}	2.80 d
Oct 1990	...	64°	H, L	Kürster & Dennerl (1993)
FK Com	FK Com	G2 III	160 km s^{-1}	2.40 d
1989	...	75°	H, L	Piskunov et al. (1994)

TABLE 1. (continued)

Star Year(s) of obs.	Type ΔV	M-K class i	$v \sin i$ Spots[1]	P_{rot} Reference
EI Eri	RS CVn	G5 IV	50 km s^{-1}	1.95 d
1984-87	0.1 mag	46°	P, L	Hatzes & Vogt (1992)
1987-88	0.15 mag	46°	P, H, L	Strassmeier et al. (1991)
V410 Tau	WTT	K4	77 km s^{-1}	1.872 d
Jan 1990	0.4 mag	70°	P	Joncour et al. (1994b)
Nov 1992	0.37 mag	70°	H, L	Strassmeier et al. (1994)
Dec 1993	0.5 mag	70°	(P), H, L	Rice & Strassmeier (1996)
1993-94	...	54°	(P), H, L	Hatzes (1995d)
HD 155555	RS CVn	K0 V-IV	29 km s^{-1}	1.68 d
Sep 1990	...	55°	P, L	Kürster et al. (1992)
LQ Hya	single	K2 V	27 km s^{-1}	1.61 d
Feb 1991	0.1 mag	70°	H, L	Strassmeier et al. (1993)
Feb 1991	...	75°	H, L	Saar et al. (1994)
May 1991	...	75°	H, L	Saar et al. (1994)
Mar 1993	...	75°	P, L	Saar et al. (1994)
HD 283572	WTT	G8 IV-V	80 km s^{-1}	1.55 d
Feb 1993	0.1 mag	60°	P	Joncour et al. (1994a)
YY Gem AB	BY Dra	dM1e	48	0.8142822 d
Feb 1993	...	87°	H, L	Hatzes (1995c)
SV Cam	RS CVn	G2V-IV	117 km s^{-1}	0.59 d
1993-94	0.07 mag	90°	H, L	Hempelmann et al. (1995)
V471 Tau	BY Dra	K2V	91 km s^{-1}	0.5211 d
1992	...	90°	P, H	Ramseyer et al. (1995)
Dec 1993	0.1 mag	90°	P, H	Ramseyer et al. (1995)
AB Dor	single	K0 V	91 km s^{-1}	0.514790 d
Feb 1989	0.1 mag	60°	H, L	Kürster et al. (1994)
Jan 1992	...	60°	P, H, L	Collier-C. & Unruh (1994)
Dec 1992	...	60°	P, H, L	Collier-Cameron (1995)
HII 3163	Pleiades	M0V	70 km s^{-1}	0.42 d
Dec 1993	...	30°	(P), H, L	Stout & Vogt (1996)
HII 686	Pleiades	K5V	64 km s^{-1}	0.397 d
Dec 1993	...	42°	(P), H, L	Stout & Vogt (1996)
AE Phe	W UMa	<G0>	?	0.3623718 d
Nov 1989	...	88°	H, L	Maceroni et al. (1994)
Nov 1990	yes	87°	H, L	Maceroni et al. (1994)
YY Eri	W UMa	<G2V>	?	0.31249510 d
Nov 1989	...	82°	H, L	Maceroni et al. (1994)
Nov 1990	yes	82°	H, L	Maceroni et al. (1994)

[1]P = Polar spot, H = High-latitude spots, L = Low-latitude spots

https://doi.org/10.1017/S0074180900083303 Published online by Cambridge University Press